HiSST: 3rd International Conference on
High-Speed Vehicle Science Technology
14 -19 April 2024, Busan, Korea

Experimental Study of Combustion Modes in PNU-DCSC with a micro-PDE

Min-Su Kim[1], Keon-Hyeong Lee[2], Eun-Sung Lee[3], Hyung-Seok Lee[4], Seung-Min Jeong[5], Bu-Kyeng Sung[6], Jeong-Yeol Choi[7]

Abstract

Scramjet engines are critical technologies for air-breathing hypersonic vehicles, with ongoing research aimed at addressing their technical challenges. Supersonic combustion in scramjet engines necessitates rapid fuel-oxidizer mixing and flame stabilization due to the short residence time in the combustor. This study presents findings from experiments conducted using the Pusan National University direct-connect scramjet combustor (PNU-DCSC) integrated with a micro-pulse detonation engine (μPDE). The experimental setup is designed for simulating flight conditions at altitudes of 20~25 km and Mach numbers of 4.0~5.0. The results show that varying the jet-to-freestream momentum flux ratio affects fuel penetration height. Furthermore, as the fuel injection pressure increases, the combustion area expands, leading to transitions in combustion modes. The flamebase, where peak combustion pressure forms, moves upstream, and pressure oscillations intensify.

Keywords: *Direct-Connect Scramjet Combustor (DCSC), Micro-Pulse Detonation Engine (μPDE), Cavity shear layer flame, Jet wake flame*

1. Introduction

Various concepts and techniques, such as the combined cycle, ram accelerator and oblique detonation wave, had been developed over the past to be applied to high-speed propulsion systems [1-10]. In recent years, there has been increasing interest in scramjet vehicle, the scramjet engine has been considered a core technology for air-breathing hypersonic vehicles, and numerous related studies have been conducted over the past several decades [11-16]. However, scramjet engines have technical issues to overcome. Essentially, supersonic combustion takes place under conditions where the flow residence time in the combustor is very short, approximately 0.1~1.0 ms, due to the high flow speed. Therefore, mixing between fuel-oxidizers must be performed rapidly, and flame stabilization technology after ignition is also required. Additionally, reliable ignition is not guaranteed under conditions where the stagnation temperature at the combustor inlet is relatively low among the hypersonic flight range. Numerous studies are in progress to practically solve problems such as mixing, ignition, and flame holding. Recent related to scramjet ignition and combustion stabilization can be classified into passive or active methods. Active methods include pulsed jet injection, pulsed detonation, and plasma intensified. As passive methods, there are geometric approaches such as cavity, and strut. In particular, the cavity can demonstrate combustion characteristics through simple shapes and numbers and can reduce the flame length and increase local heat release through recirculation zones and shear layers, so they have been applied as flame holders [17-19].

[1] *Department of Aerospace Engineering, Pusan National University, Busan 46241, Korea, rotation17@naver.com*
[2] *Department of Aerospace Engineering, Pusan National University, Busan 46241, Korea, khl1903@naver.com*
[3] *Department of Aerospace Engineering, Pusan National University, Busan 46241, Korea, tony89s@naver.com*
[4] *Department of Aerospace Engineering, Pusan National University, Busan 46241, Korea, hanhseok@naver.com*
[5] *Aeropropulsion Research Division, Korea Aerospace Research Institute, Daejeon 34133, Korea, smjeong@kari.re.kr*
[6] *Department of Aerospace Engineering, Pusan National University, Busan 46241, Korea, tjdqnrud91@naver.com*
[7] *Department of Aerospace Engineering, Pusan National University, Busan 46241, Korea, aerochoi@pusan.ac.kr*

The supersonic combustion facility used in this study is constructed by direct-connecting a small rocket combustor type vitiated air heater (VAH) and a scramjet combustor. The blowdown type heat generation facility supplies vitiated air adequate for a lab-scale direct-connect scramjet combustor. The operation time is an order of seconds, and the cost per test is low, minimizing the facility scale.

In this study, we present the characteristics of a scramjet combustor utilizing μPDE. The μPDE single pulse shot was applied. Also, combustion characteristics resulting from changes in fuel injection pressure and corresponding equivalence ratio were confirmed in the scramjet combustor of the baseline model. The results are expected to serve as reference data for parametric studies that will be performed by changing various variables that can be considered in scramjet combustors.

2. Experimental apparatus

2.1. Pusan National University Direct-Connect Scramjet Combustor

The Pusan National University direct-connect scramjet combustor (PNU-DCSC) constructed and utilized in this study consists of a gas supply system, VAH, isolator, and scramjet combustor as shown in Figure 1. The target design point corresponds to an altitude of 20~25 km and a flight Mach number of 4.0~5.0. High enthalpy vitiated air with a total pressure 1.731 MPa and a total temperature of 1610 K is supplied to the isolator through the circular to rectangular shape transition (CRST) nozzle. As a result, due to the isentropic relationship, the static pressure of 0.225 MPa, static temperature of 1000 K, and Mach number of 2.0 are satisfied at the CRST nozzle exit [20-22]. The total mass flow rate and chemical composition of vitiated air are shown in Table 1. The VAH exit Mach number verification test using a tungsten wedge was performed as a prior experimental study [23,24].

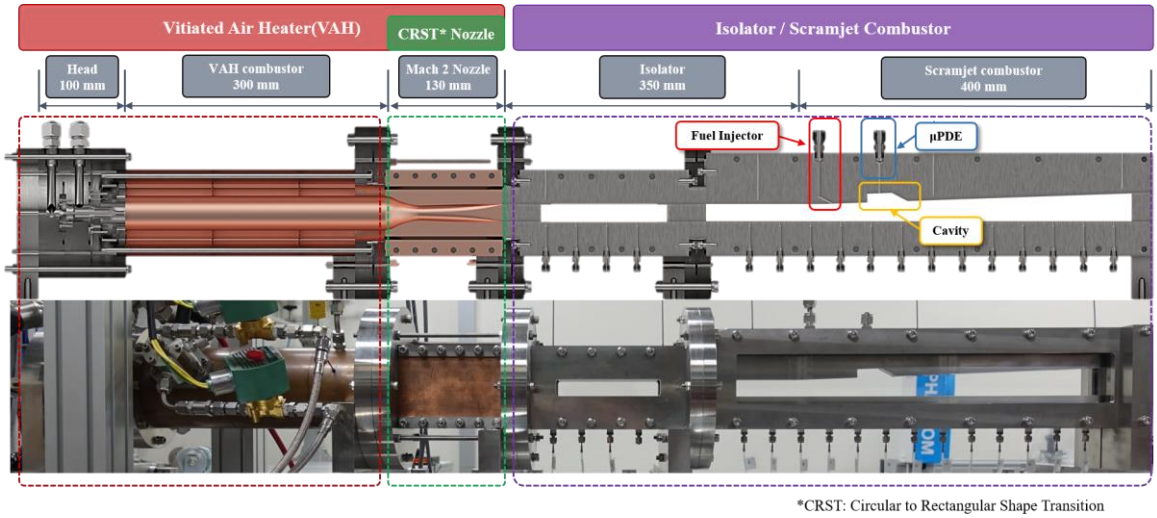

Fig 1. Configuration of PNU-DCSC

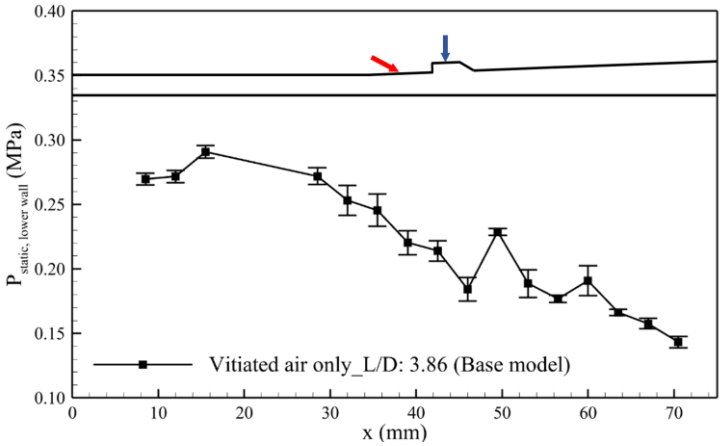

Fig 2. Wall pressure of isolator-scramjet combustor with only vitiated air

Table 1. Condition of vitiated air corresponding to the design point

Chemical composition				Exit of CRST nozzle		
χ_{O_2}	χ_{N_2}	χ_{H_2O}	$\dot{m}_{total}$ g/s	P_e MPa	T_e K	M
21.0	58.5	20.5	369.99 ± 7.09	0.226	1000	2.04 ± 0.04

The width and height of the isolator are 20 mm and have the same square cross-section, followed by a scramjet combustor with a divergence angle of 2°. The outlet of the fuel injector is 30 mm away from the starting point of the combustor and has an elliptic shape because the gaseous hydrogen fuel is injected at an angle of 30°. The leading edge of the cavity is 70 mm away from the combustor starting point, and the dimensions are as follows: bottom length = 30 mm, depth = 10 mm, ramp angle = 30°. The results of VAH initiation after directly connecting the isolator and scramjet combustor are shown in Figure 2.

2.2. Micro-Pulse Detonation Engine

The μPDE is installed on the external upper wall of the scramjet combustor. It is located at the center of the cavity floor, as depicted in Figure 3, and referred Han et al.'s model [25]. The diameter of the μPDE is 4.22 mm and the length is 200 mm. Fuel of GH2 and oxidizer of GO2 were injected with a total mass flow rate of 5.52 g/s, equivalence ratio of 1.82 and ignited by a spark plug. The total mass flow rate of μPDE is only 1.5% of the vitiated air. To avoid partial filling, the fuel-oxidizer valve control time was set to 40 ms, which takes into account the delay time of the solenoid valve. Additionally, it is ignited 30 ms after the start of valve control by the spark plug. From the results of a single shot ignition as shown in Figure 3, it is possible to observe the detonation entering the supersonic combustor. Detonation appears in a coupled but swiftly decouples within a short duration.

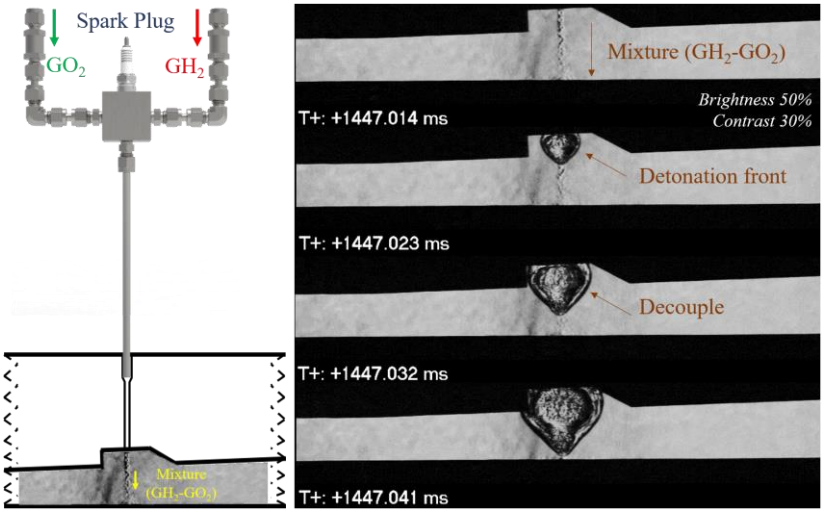

Fig 3. Configuration of μPDE: (Left) Installation of μPDE (Right) Single-shot result of μPDE

2.3. Test condition and sequence

The cases performed in this study are shown in Table 1. The flow rate and time of the mixture supplied to the μPDE were excessively small compared to vitiated air, so they were not considered in the global equivalence ratio (Φ) of the scramjet combustor. When 40 ms was supplied, the flow rate from the μPDE was only 0.22 g/s. In all cases, auto-ignition did not occur, primarily due to the static temperature of 1,000 K in the inlet of isolator. This represented conditions where auto-ignition was difficult to occur

with hydrogen fuel. So, the μPDE was used as an ignitor through single-shot operation. When using the μPDE as an ignitor, successful ignition was achieved in all cases. The μPDE provided sufficient high-temperature, high-pressure radicals for ignition, demonstrating potential as an ignitor for scramjet engines.

The automatic sequence applied to perform the combustion test is shown in Figure 4 and is follows: GH_2 and GO_2 are fed into the combustion chamber for VAH and ignited by combustion wave ignitor (CWI). Immediately after, air is supplied and the pressure in the VAH combustion chamber begins to rise. During the entire test, the pressure inside the VAH chamber reaches a steady state within 1.0 s. Afterwards, GH_2 fuel is injected into the scramjet combustor. At 1.4 s, μPDE subsystem control is applied. Finally, after the single pulse shot of the μPDE, the experiment ends at 2.4 s.

Table 2. Set fuel supply and resulting scramjet combustor conditions

Case	Scramjet combustor		
	P_{fuel} MPa	$\dot{m}_{fuel}$ g/s	Φ
1	1.077 ± 0.026	1.194 ± 0.036	0.109 ± 0.001
2	1.611 ± 0.007	1.956 ± 0.061	0.179 ± 0.008
3	2.613 ± 0.004	3.411 ± 0.091	0.308 ± 0.004
4	3.613 ± 0.002	4.541 ± 0.123	0.426 ± 0.022
5	4.619 ± 0.006	5.922 ± 0.107	0.551 ± 0.012

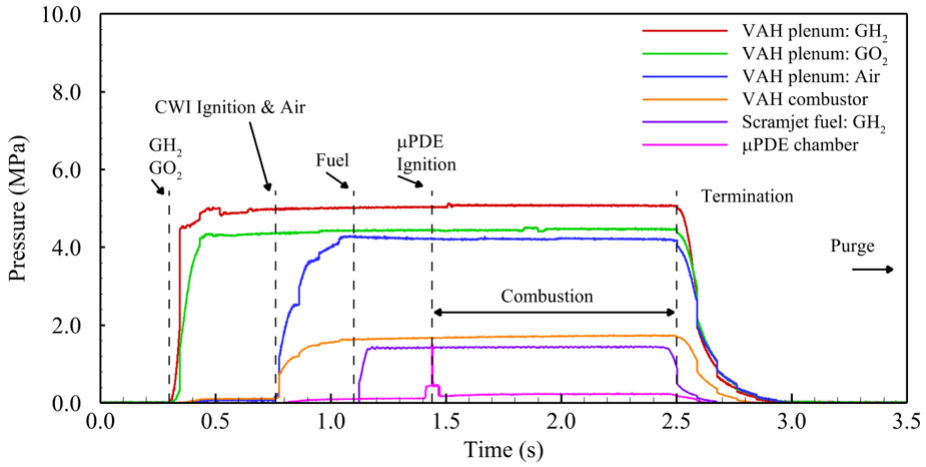

Fig 4. Test sequence for scramjet combustor

3. Result and discussion

3.1. Characteristics of inclined injector

In the case of a wall hole-type injector in a scramjet engine, there are generally two types of injection: transverse and inclined injection. The difference between the two methods. The transverse injection method acts as a barrier to the freestream and generates a strong bow shock. This creates a back pressure gradient, separating the boundary layer of the fuel jet and forming a high-pressure region with a recirculation zone below the boundary layer. A low-pressure area is formed downstream of the jet, and a recirculation zone is created by the flow flowing into that area. In this way mixing of the supersonic flow is improved. However, transverse injectors cause a total pressure loss due to the strong bow shock caused by fuel jet penetration. To alleviate this, an inclined injection method may contribute

to increasing thrust efficiency by increasing the axial momentum of the fuel jet. However, this method is disadvantageous for auto ignition of a scramjet combustor [26-32].

In fact, based on the test sequence, auto ignition did not occur within 1.0~1.4 s. As mentioned earlier, this can be expected to be caused by the low inlet stagnation temperature and characteristics of inclined injection. Table 3 shows the jet to freestream momentum flux ratio (J) according to fuel injection conditions calculated through equation (1).

$$J = \frac{(\rho u^2)_j}{(\rho u^2)_\infty} = \frac{(\gamma P M^2)_j}{(\gamma P M^2)_\infty} \tag{1}$$

Table 3. Jet to freestream momentum flux ratio calculation (J)

Case	J
1	0.195 ± 0.007
2	0.314 ± 0.017
3	0.550 ± 0.020
4	0.733 ± 0.024
5	0.958 ± 0.023

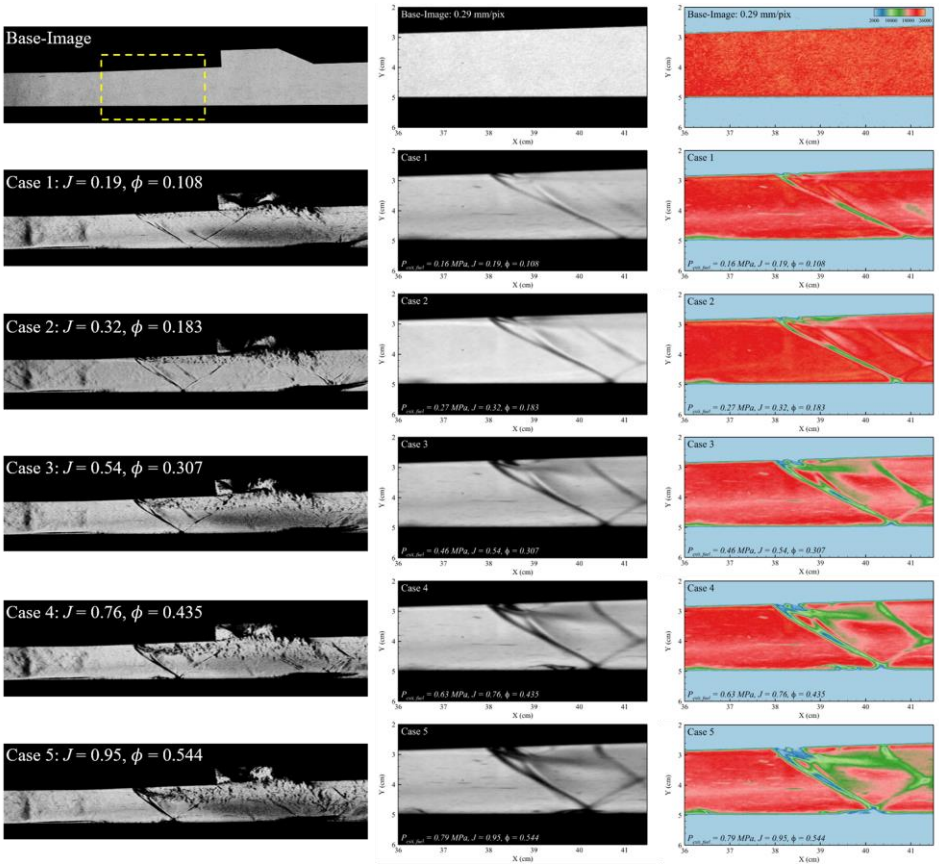

Fig 5. Fuel jet stream: (Left) Instantaneous (Mid) Time-averaged in gray scale (Right) Time-averaged in color scale

Figure 5 shows images showing injection characteristics according to fuel supply conditions along with the base-image when the experiment was not performed. In order to check the characteristics of the fuel jet in detail, some areas were enlarged and used as shown in the yellow dashed box in the base-image. The instantaneous and time-averaged flow field were confirmed together. In addition, images of color scale were expressed together for visibility. The instantaneous image was taken at 1.4 s, and the time-averaged image consisted of 11031 snapshots spanning 1.3~1.4 s.

Unlike the transverse injection method, upstream of the fuel jet plume, the recirculation zone was barely developed, and was formed only very narrowly even when the injection pressure increased. On the other hand, as the injection pressure increases downstream of the plume, a low-pressure recirculation zone clearly develops. As a result, it can be seen that as the injection pressure and J increases, the recirculation zone develops downstream of the fuel jet plume and the jet penetration height improves.

3.2. Combustion Characteristics: Wall pressure and FFT analysis

An attempt was made to forcibly initiate the scramjet combustor by applying μPDE subsystem operation and single pulse shot immediately after 1.4 s to the supersonic flow in which auto ignition did not occur. In all cases, not only was ignition reliable, but flame holding and combustion continued until the end of the test. After the initial ignition, a pressure distribution showing a certain trend was formed around 1.5 s. Figure 6 shows the time-averaged pressure distribution for 1.6~2.4 s for each case. The wall static pressure was measured using scanivalve, a 16 channels pressure scanner, with a sampling rate of 500 Hz.

The location of peak pressure due to combustion changed depending on the equivalence ratio (Φ), and as the Φ increased, the pressure upstream of the combustor and in the isolator also increased. In addition, as the pressure distribution upstream of the combustor increased, the pressure fluctuation over time changed and the area where the trend was visible expanded in the longitudinal direction.

Figure 7 shows the pressure history over time in the range of 1.6~2.4 s for all cases and the Fast Fourier Transform (FFT) results for each case. Corresponds to the results of case 1~5 in order from top to bottom. The black and mint solid lines correspond to regions other than the main frequency region where the amplitude was measured to be relatively high. This is summarized in Table 4.

As a result, the location of peak pressure due to combustion and the area where the main frequency was confirmed to have the relatively high amplitude were identical in case 1 and case 2, respectively, but were different in case 3, case 4, and case 5. This can be inferred that the causes and phenomena (e.g. instability) of major frequencies that appear depending on the global equivalence ratio may be different.

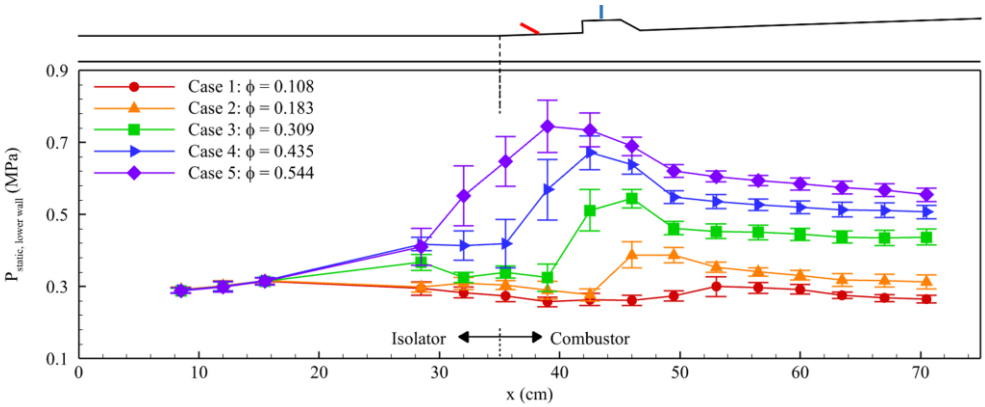

Fig 6. Time-averaged wall static pressure distribution

Table 4. Comparison of peak pressures and major frequency ranges

Case	1	2	3	4	5
Location of peak pressure (cm)	53.0	46.0	46.0	42.5	39.0
Location of major frequency (cm)	53.0	46.0	42.5	39.0	32.0, 39.0

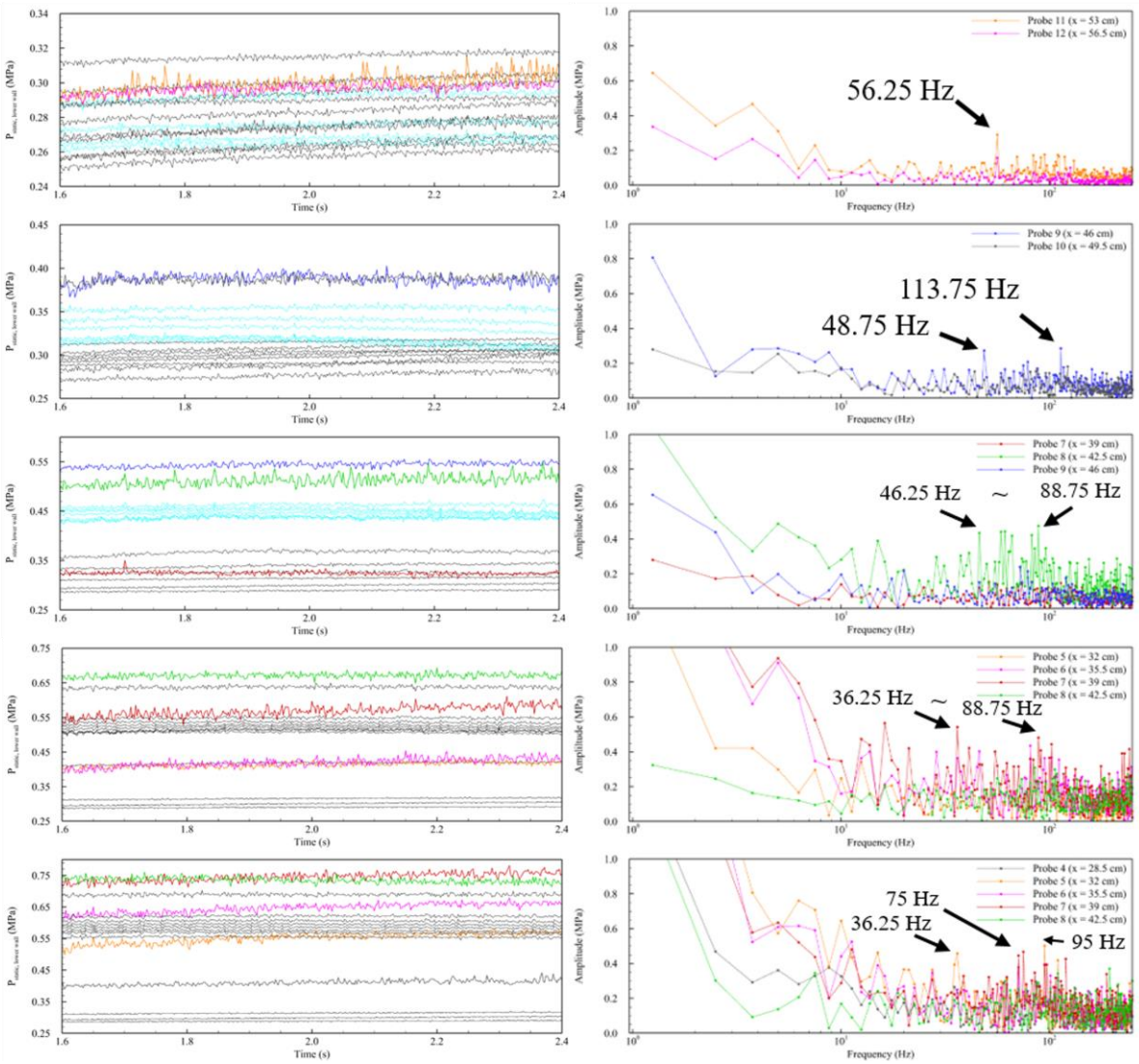

Fig 7. (Left) Wall static pressure history (Right) FFT results

3.3. Combustion Characteristics: High-speed images and DMD analysis

For detailed analysis of combustion characteristics, Schlieren, which shows the shock wave structure and combustion flow field due to density gradient, and flame luminosity to determine the intensity and dynamic characteristics of the flame were used. The phantom v2512 high-speed camera used. Acquisition conditions are common to both Schlieren and flame, corresponding to a resolution of 1024 $\times$ 208 and a sample rate of 110 kHz. The exposure rate is 0.8 μs for Schlieren and 4.0 μs for flame, respectively. Instantaneous and time-averaged images were used as shown in Figure 8 and Figure 9, and sub-modes using dynamic mode decomposition (DMD) were presented as shown in Figure 10 [33].

In case 1, only the bow shock and reflected shock caused by fuel injection appeared. In case 2, as the Φ increased, an oblique shock wave anchored at the leading edge of the cavity began to develop (pre-combustion shock wave), and oblique shock waves following it were observed as phenomena such as formation, dissipation, and oscillation along the combustion area. In both cases, the flame was diffused from the cavity along the shear layer and was classified as a cavity shear layer flame.

In case 3, as in the previous cases, a flame was formed from the leading edge of the cavity, but the area increased in the transverse direction, and a shock train accompanied by a λ type pre-combustion shock wave was formed. This resulted in longitudinal oscillation in the area between the fuel injector and the cavity, along with a transverse expansion of the combustion area. It was classified as a cavity flame.

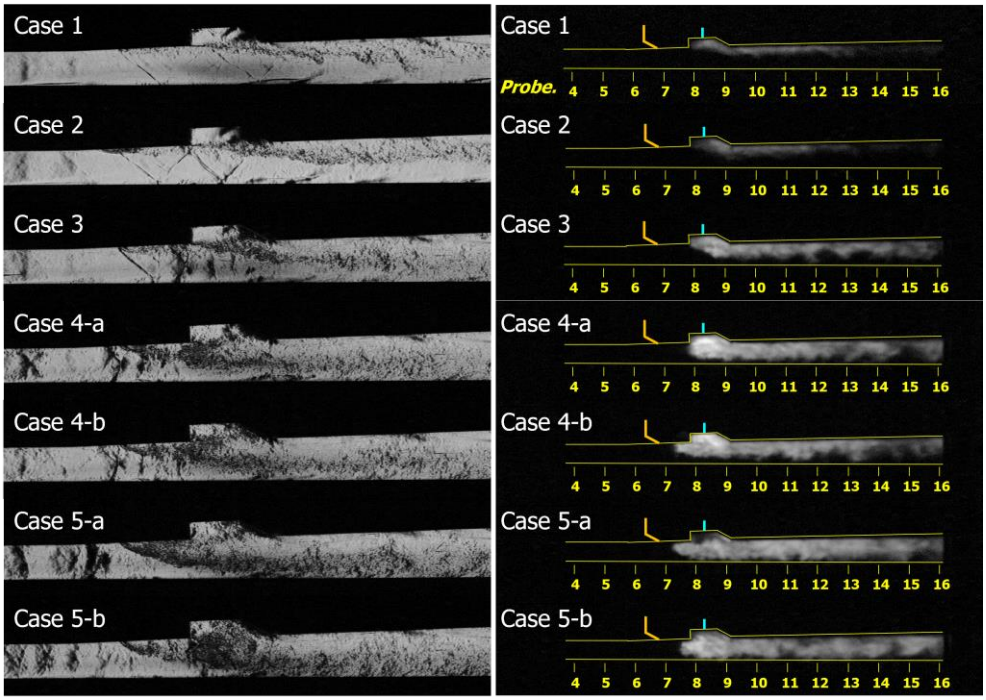

Fig 8. Instantaneous: (Left) Schlieren (Right) Flame luminosity

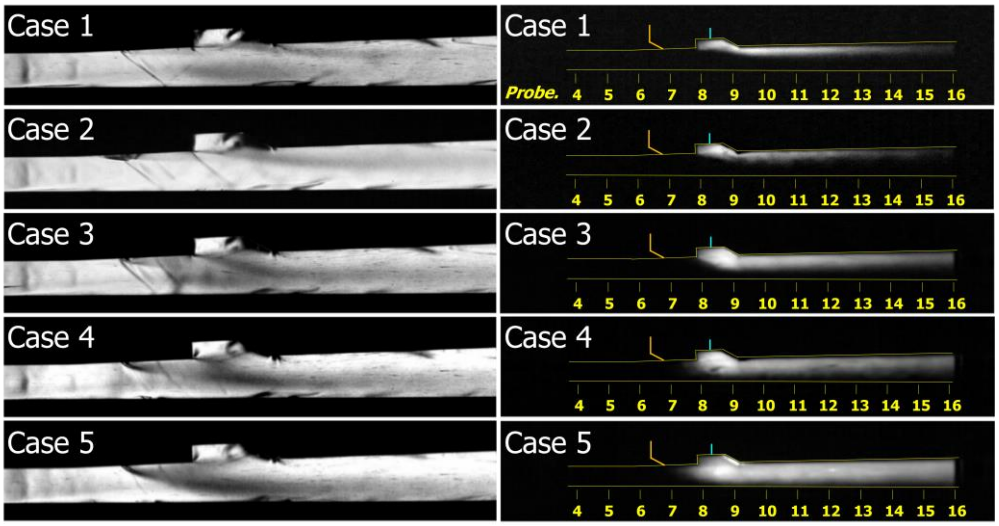

Fig 9. Time-averaged: (Left) Schlieren (Right) Flame luminosity

Starting from case 4, the flame was not anchored to the cavity and shear layer. In addition, it intermittently spread to the area between the fuel injector and the leading edge of a cavity, showing instability. Shock trains were also repeatedly observed to propagate, expand, and oscillate up to the combustor entrance. In other words, it became unstable due to increased heat release and thermal choking. Although the shock train intermittently extended downstream of the isolator, the range where instability due to oscillation was predominantly confirmed did not extend beyond the entrance of the supersonic combustor. This can also be seen through the sub mode of case 4 in Figure 10. In case 3, the area where the shock train's dynamic characteristics appear was very limited near the cavity, but in case 4, it expanded upstream of the fuel injector and developed further, and the flame was not fixed to the cavity. Due to this clear difference, it was distinguished as a lifted jet flame.

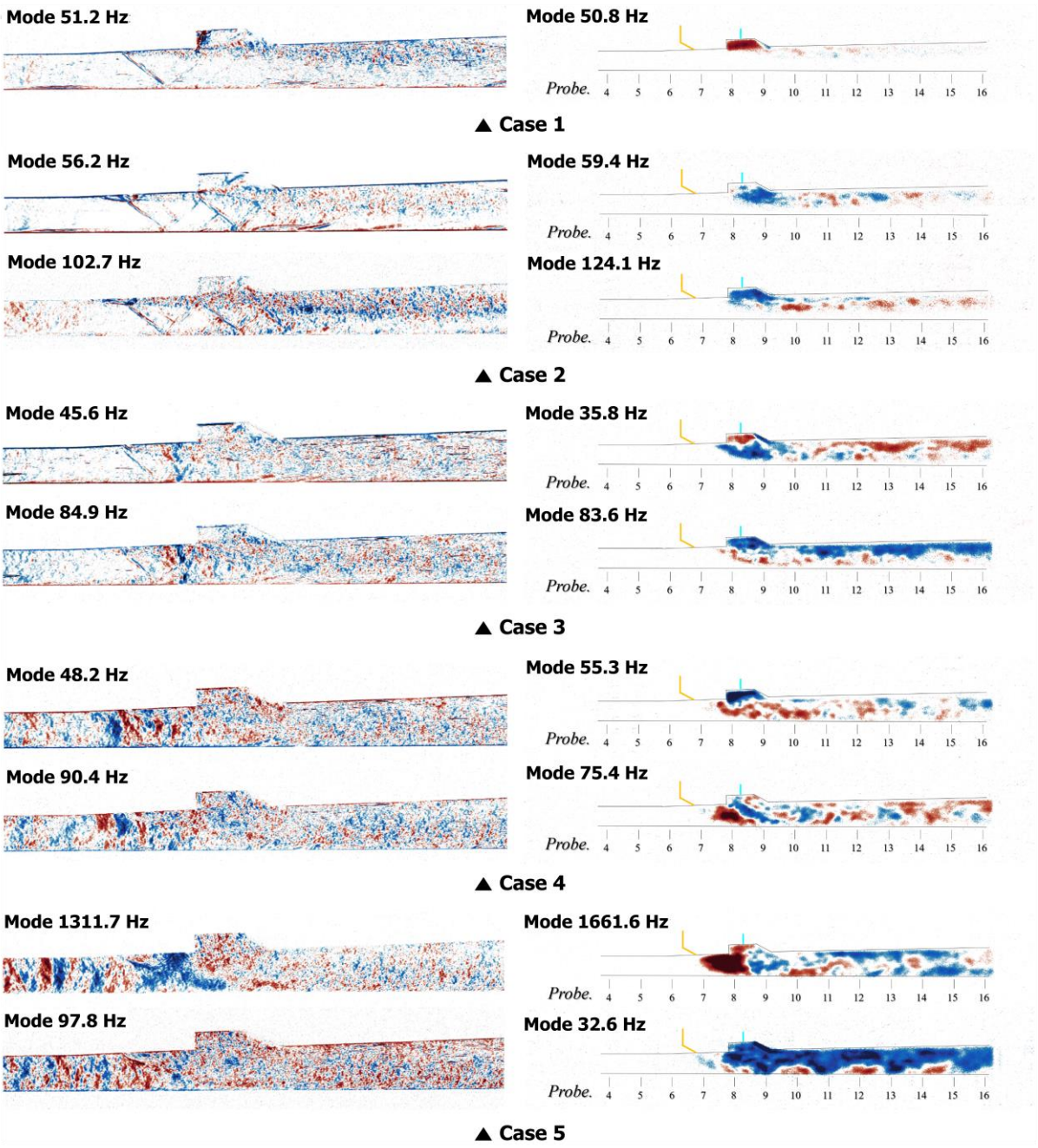

Fig 10. Sub-mode: (Left) Schlieren (Right) Flame luminosity

As the Φ increases as in case 5, shock train extends to the isolator, and the dominant flame region expands to the fuel injector. Additionally, as the Φ increased, normal shock appeared due to the gradient caused by rapid heat release in the combustion area and spread to some areas of the isolator (upstream traveling shock wave, UTSW) [34,35]. In this case, longitudinal instability in the overall combustion region and dominant instability behind the fuel injector were confirmed in the sub mode above 1 kHz. Longitudinal oscillation and instability caused by the shock train were also seen, but it was not possible to discern how far the area of the shock train extended in the upstream direction beyond the imaging range, and it was difficult to clearly distinguish instability in the sub mode below 100 Hz. Therefore, Schlieren images of the isolator area were additionally taken and analyzed as shown in Figure 11.

Fig 11. Isolator-scramjet combustor results in case 5: (Left) Instantaneous snapshots of shock train and UTSW (Right) sub-mode

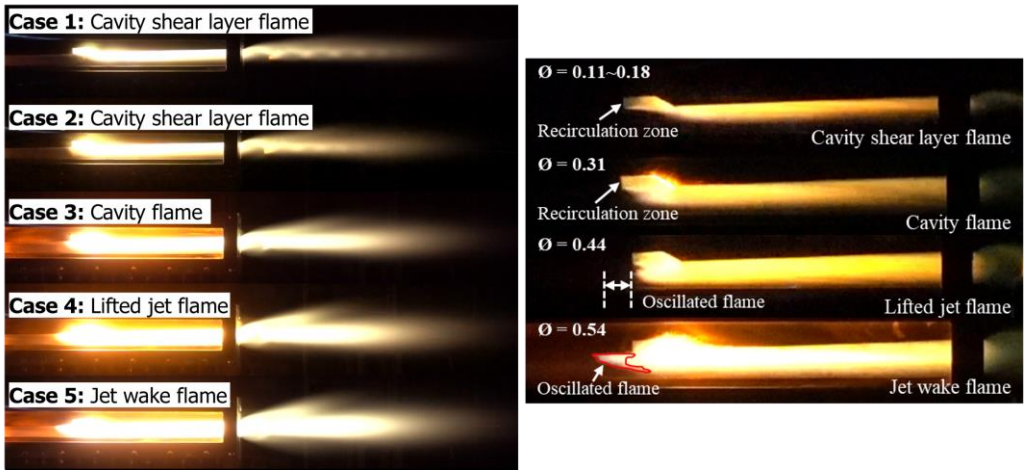

Fig 12. Digital camera snapshots of all cases

Through this, we were able to observe not only the expansion and oscillation of the shock train, but also phenomena such as UTSW. Because of these characteristics, it was further classified as a jet wake flame accompanied by propagation of normal shock. Figure 12 is a snapshot of digital camera showing the experimental results for all cases.

4. Conclusion

Based on the scramjet ground experiment facility at Pusan National University, supersonic combustor experiments were conducted. This experiment utilized a single angle hole injector, and combustion tests were carried out with varying injection pressure. The penetration distance of the fuel injected from the inclined injector before ignition was examined using Schlieren images. The fuel jet injected at an inclined angle did not affect the upstream direction, but created a recirculation zone in the downstream direction. As the injection pressure increased, the penetration height also increased. The ignition of the supersonic combustor was conducted using the μPDE. The equivalence ratio of the supersonic combustor was varied according to the injection pressure, and the various combustion modes were observed. In particular, the flame area significantly expanded in the lifted jet wake flame and jet wake flame combustion modes, with pronounced longitudinal instability. Intense heat release resulted in thermal choking, and its phenomena propagated further upstream than the position of the injector. In future research, it is expected that the application of multi pulse shot using μPDE and active control of the combustion mode will be possible.

References

1. Choi, J.-Y., Jeung, I.-S., Yoon, Y.: Unsteady-state simulation of model ram accelerator in expansion tube. AIAA Journal, 37(5), 537–543 (1999) https://doi.org/10.2514/2.770
2. Choi, J.-Y., Jeung, I.-S., Yoon, Y.: Scaling effect of the combustion induced by shock-wave boundary-layer interaction in premixed gas. Symposium (International) on Combustion, 27(2), 2181–2188 (1998) https://doi.org/10.1016/S0082-0784(98)80067-2
3. Choi, J.-Y., Jeung, I.-S., Lee, S.: Dimensional analysis of the effect of flow conditions on shock-induced combustion. Symposium (International) on Combustion, 26(2), 2925–2932 (1996) https://doi.org/10.1016/S0082-0784(96)80134-2
4. Pavalavanni, P.K., Sohn, C.H., Lee, B.J., Choi, J.-Y.: Revisiting unsteady shock-induced combustion with modern analysis techniques. Proceedings of the Combustion Institute, 37(3), 3637–3644 (2019) https://doi.org/10.1016/j.proci.2018.07.094
5. Kim, S.-L., Choi, J.-Y., Jeung, I.-S., Park, Y.-H.: Application of approximate chemical Jacobians for constant volume reaction and shock-induced combustion. Applied Numerical Mathematics, 39(1), 87–104 (2001) https://doi.org/10.1016/S0168-9274(01)00054-X
6. Kumar, P.P., Kim, K.-S., Oh, S., Choi, J.-Y.: Numerical comparison of hydrogen-air reaction mechanisms for unsteady shock-induced combustion applications. J. of Mechanical Science and Technology, 29(3), 893–898 (2015) https://doi.org/10.1007/s12206-015-0202-2
7. Choi, J.-Y., Han, S.-H., Kim, K.H., Yang, V.: High resolution numerical study on the coaxial supersonic turbulent flame structures. 50th AIAA/ASME/SAE/ASEE Joint Propulsion Conference 2014 (2014) https://doi.org/10.2514/6.2014-3745
8. Choi, J.-Y., Unnikrishnan, U., Hwang, W.-S., Jeong, S.-M., Han, S.-H., Kim, K. H, Yang, V.: Effect of fuel temperature on flame characteristics of supersonic turbulent combustion. Fuel, 329, 125310 (2022) https://doi.org/10.1016/j.fuel.2022.125310
9. Kim, H.-S., Oh, S., Choi, J.-Y.: Quasi-1D analysis and performance estimation of a sub-scale RBCC engine with chemical equilibrium. Aerospace Science and Technology, 69, 39–47 (2017) https://doi.org/10.1016/j.ast.2017.06.019
10. Kim, H.-S., Kim, K.-S., Oh, S.-J., Choi, J.-Y., Yang, W.-S.: A preliminary design of flight test conditions for a sub-scale RBCC engine using a sounding rocket. International J. of Aeronautical and Space Sciences, 16(4), 529–536 (2015) https://doi.org/10.5139/IJASS.2015.16.4.529
11. Choi, J.-Y., Noh, J., Byun, J.-R., Lim, J. S., Togai, K., Yang, V.: Numerical investigation of combustion/shock-train interactions in a dual-mode scramjet engine, 17th AIAA International Space Planes and Hypersonic Systems and Technologies Conference 2011 (2011) https://doi.org/10.2514/6.2011-2395

12. Vyasaprasath, K., Oh, S., Kim, K.-S., Choi, J.-Y.: Numerical studies of supersonic planar mixing and turbulent combustion using a detached eddy simulation (DES) model. International J. of Aeronautical and Space Sciences, 16(4), 560–570 (2015) https://doi.org/10.5139/IJASS.2015.16.4.560

13. Won, S.-H., Jeung, I.-S., Choi, J.-Y.: Turbulent combustion characteristics in HyShot model combustor with transverse fuel injection. 43rd AIAA/ASME/SAE/ASEE Joint Propulsion Conference, AIAA4124–4135 (2007) https://doi.org/10.2514/6.2007-5427

14. Choi, J.-Y., Yang, V., Ma, F., Won, S.-H., Jeung, I.-S.: Detached Eddy simulation of combustion dynamics in scramjet combustors. 43rd AIAA/ASME/SAE/ASEE Joint Propulsion Conference, 1, 231–237 (2007) https://doi.org/10.2514/6.2007-5027

15. Choi, J.-Y., Yang, V., Fuhua, M., Won, S.-H., Jeung, I.-S.: DES Modeling of Supersonic Combustion in Scramjet Combustors. AIAA/ASME/SAE/ASEE 42nd Joint Propulsion Conference, 9 (2006) https://doi.org/10.2514/6.2006-5097

16. Jeong, S.-M., Choi, J.-Y.: Combined diagnostic analysis of dynamic combustion characteristics in a scramjet engine. Energies, 13(15), 4029 (2020) https://doi.org/10.3390/en13154029

17. Liu Q, Baccarella D, Lee T.: Review of combustion stabilization for hypersonic airbreathing propulsion. Progress in Aerospace Sciences. 119, 100636 (2020) https://doi.org/10.1016/j.paerosci.2020.100636

18. Yu, K. H., Wilson, K. J., Schadow, K. C.: Effect of flame-holding cavities on supersonic-combustion performance. Journal of Propulsion and Power, 17(6), 1287-1295 (2001) https://doi.org/10.2514/2.5877

19. Kim, M.-S., Koo, I.-H., Lee, K.-H., Lee, E.-S., Han, H.-S., Jeong, S.-M., Choi, J.-Y.: Experimental Study on the Ignition Characteristics of Scramjet Combustor with Tandem Cavities Using Micro-Pusle Detonation Engine. Aerospace, 10(8), 706 (2023) https://doi.org/10.3390/aerospace10080706

20. Sung, B.-K., Jeong, S.-M., Choi, J. Y.: Direct-connect supersonic nozzle design considering the effect of combustion. Aerospace Science and Technology, 133, 108094 (2023) https://doi.org/10.1016/j.ast.2022.108094

21. Sung, B.-K., Choi, J.-Y.: Design of a Mach 2 shape transition nozzle for lab-scale direct-connect supersonic combustor. Aerospace Science and Technology. 117, 106906 (2021) https://doi.org/10.1016/j.ast.2021.106906

22. Sung, B.-K., Hwang, W.-S., Choi, J.-Y.: Design of a Shape Transition Nozzle for Lab-scale Supersonic Combustion Experimental Equipment. J. of the Korean Society for Aeronautical and Space Sciences, 48(3), 207–215 (2020) https://doi.org/10.5139/JKSAS.2020.48.3.207

23. Lee, J.-H., Lee, E.-S., Han, H.-S., Kim, M.-S., Choi, J.-Y.: A Study on a Vitiated Air Heater for a Direct-Connect Scramjet Combustor and Preliminary Test on the Scramjet Combustor Ignition. Aerospace, 10(5), 415 (2023)

https://doi.org/10.3390/aerospace10050415

24. Lee, E.-S., Han, H.-S., Lee, J.-H., Choi, J.-Y.: A Study on the Flow Conditions of the Combustion Air Heater Outlet for the Supersonic Combustion Experiment. Journal of the Korean Society of Propulsion Engineers, 26(1), 88097 (2022) https://doi.org/10.6108/KSPE.2022.26.1.088

25. Han, H.-S., Kim, J.-M., Oh, S., Choi, J.-Y.: An Experimental Study on Characteristics of Small-scale PDE under Low-frequency Operating Conditions. Journal of the Korean Society of Propulsion Engineers, 22(3), 81-89 (2018) https://doi.org/10.6108/KSPE.2018.22.3.081

26. Ben-Yakar, A.: Experimental investigation of mixing and ignition of transverse jets in supersonic crossflows. Stanford University (2001)

27. Gruber, M.R., Nejad, A.S., Chen, T.H., Dutton, J. C.: Mixing and Penetration Studies of Sonic

Jets in a Mach 2 Freestream. Journal of Propulsion and Power, 11(2), 315-323 (1995) https://doi.org/10.2514/3.51427

28. Gerdroodbary, M. B.: Scramjets: fuel mixing and injection systems. Butterworth-Heinemann (2020)
29. Choi, J.-Y., Ma, F., Yang, V.: Dynamics combustion characteristics in scramjet combustors with transverse fuel injection. 41st, AIAA/ASME/SAE/ASEE Joint Propulsion Conference and Exhibit (2005) https://doi.org/10.2514/6.2005-4428
30. Won, S.-H., Jeung, I.-S., Shin, J.-R., Cho, D.-R., Choi, J.-Y.: Three-dimensional dynamic characteristics of transverse fuel injection into a supersonic cross flow. 15th AIAA International Space Planes and Hypersonic Systems and Technologies Conference, 2008-2515 (2008) https://doi.org/10.2514/6.2008-2515
31. Won, S.-H., Jeung, I.-S., Choi, J.-Y.: DES study of transverse jet injection into supersonic cross Flows. 44th AIAA Aerospace Sciences Meeting, 20, 14908–14915 (2006) https://doi.org/10.2514/6.2006-1227
32. Won, S.-H., Jeung, I.-S., Choi, J.-Y.: DES investigation of the ignition of hydrogen transverse jet into high enthalpy supersonic crossflow, 47th AIAA Aerospace Sciences Meeting including the New Horizons Forum and Aerospace Exposition, 2009-1557 (2009) https://doi.org/10.2514/6.2009-1557
33. Schmid, P. J.: Dynamic mode decomposition of numerical and experimental data. Journal of fluid mechanics, 656, 5-28 (2010) https://doi.org/10.1017/S0022112010001217
34. Jeong, S.-M., Lee, J.-H., Choi, J.-Y.: Numerical investigation of low-frequency instability and frequency shifting in a scramjet combustor. Proceedings of the Combustion Institute, 39(3), 3107-3116 (2023) https://doi.org/10.1016/j.proci.2022.07.245
35. Jeong, S.-M., Han, H.-S., Sung, B.-K., Kim, W., Choi, J.-Y.: Reactive Flow Dynamics of Low-Frequency Instability in a Scramjet Combustor. Aerospace, 10(11), 932 (2023) https://doi.org/10.3390/aerospace10110932